

Predicting Change, Not States: An Alternate Framework for Neural PDE Surrogates

Anthony Zhou^{1*} and Amir Barati Farimani^{1,2*}

¹Department of Mechanical Engineering, Carnegie Mellon University, Pittsburgh, PA, USA.

²Machine Learning Department, Carnegie Mellon University, Pittsburgh, PA, USA.

*Corresponding author(s). E-mail(s): ayz2@andrew.cmu.edu; barati@cmu.edu;

Abstract

Neural surrogates for partial differential equations (PDEs) have become popular due to their potential to quickly simulate physics. With a few exceptions, neural surrogates generally treat the forward evolution of time-dependent PDEs as a black box by directly predicting the next state. While this is a natural and easy framework for applying neural surrogates, it can be an over-simplified and rigid framework for predicting physics. In this work, we propose an alternate framework in which neural solvers predict the temporal derivative and an ODE integrator forwards the solution in time, which has little overhead and is broadly applicable across model architectures and PDEs. We find that by simply changing the training target and introducing numerical integration during inference, neural surrogates can gain accuracy and stability. Predicting temporal derivatives also allows models to not be constrained to a specific temporal discretization, allowing for flexible time-stepping during inference or training on higher-resolution PDE data. Lastly, we investigate why this new framework can be beneficial and in what situations does it work well.

Keywords: machine learning, partial differential equations, neural surrogates, numerical methods

1 Introduction

Partial differential equations (PDEs) model a wide variety of physical phenomena, from neuron excitations to fluid flows to climate patterns. Many of the most complex yet practically relevant PDEs are time-dependent and can be expressed in the form:

$$\frac{\partial \mathbf{u}}{\partial t} = F(t, \mathbf{x}, \mathbf{u}, \frac{\partial \mathbf{u}}{\partial x}, \frac{\partial^2 \mathbf{u}}{\partial x^2}, \dots) \quad t \in [0, T], \mathbf{x} \in \Omega \quad (1)$$

Where there is one time dimension $t = [0, T]$ and multiple spatial dimensions $\mathbf{x} = [x_1, x_2, \dots, x_D]^T \in \Omega$, and $\mathbf{u} : [0, T] \times \Omega \rightarrow \mathbb{R}^{d_p}$ is a quantity that is solved for with a physical dimension d_p .

Solving equations of this form are of great interest, motivating centuries of research and leading to many modern engineering and scientific advances. Although solutions are analytically intractable, solutions can be approximated by discretizing the domain, where $t_n \in \{t_0, \dots, t_N\}$, $x_m \in \{x_0, \dots, x_M\}$, and the solution $\mathbf{u}(t_n, x_m)$ is discretized in this domain. Within this setup, initial conditions $\mathbf{u}(0, x_m)$ and boundary conditions $B[\mathbf{u}](t_n, x_b), x_b = \{x_m : x_m \in \partial\Omega\}$ are usually given based on the practical application of the PDE.

Numerical Solvers. Within this setup, numerical solvers are the dominant approach to approximating PDE solutions. In general, numerical solvers aim to compute \mathbf{u} by calculating an approximation of $\frac{\partial \mathbf{u}}{\partial t}|_{t=t_n} \approx F(t_n, \mathbf{u}(t_n))$ and evolving the current solution forward in time using this temporal derivative.

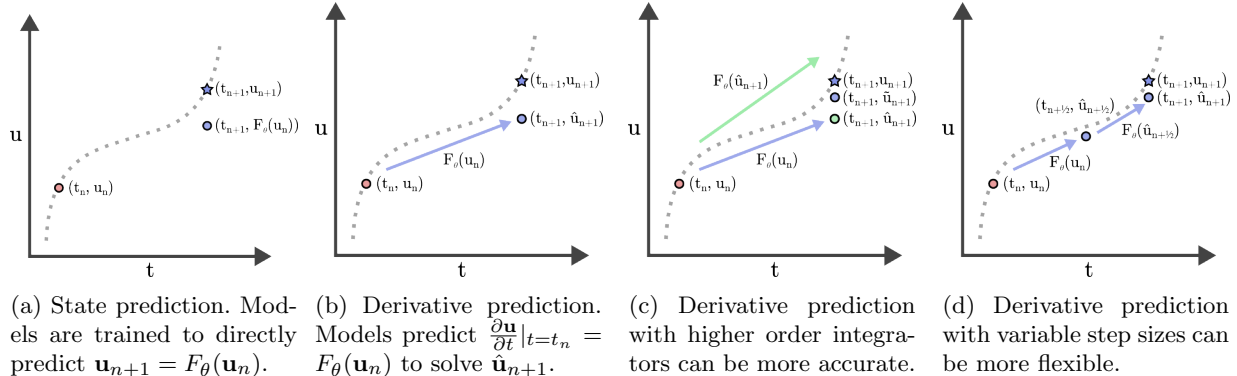


Fig. 1: A comparison of state prediction and derivative prediction, where models are either trained to predict \mathbf{u}_{n+1} or $\frac{\partial \mathbf{u}}{\partial t}|_{t=t_n}$. During inference, models are given an initial solution \mathbf{u}_n , and predict future solutions along the dashed trajectory. By predicting the temporal derivatives rather than the future solution, derivative prediction can learn spatial updates while an ODE integrator updates the solution in time, which can improve accuracy. Furthermore, derivative prediction can use higher-order integrators or variable timesteps, which further improves its accuracy and flexibility, while being applicable across model architectures and datasets.

This temporal derivative can be approximated by discretizing the spatial derivatives at the current time, such as using finite-difference or finite-element methods. In the most straightforward case, constructing this approximation converts the PDE into an ODE, which allows the solution to be evolved forward in time with an ODE integrator such as forward Euler or Runge-Kutta, also known as the method of lines [1]. Complex PDEs may require a more careful treatment of the temporal update, such as splitting the update into an intermediate timestep [2]. As a whole, both the temporal and spatial approximation require a disciplined and informed choice in discretization schemes (explicit/implicit, 1st-order/2nd-order, triangle/quad elements, etc.); importantly, the resulting accuracy, convergence, and solution time are all influenced by these choices.

Neural Surrogates. As a result, deriving and solving an accurate approximation of \mathbf{u} can require significant technical expertise and computational resources. This has motivated a new class of deep learning methods, or *neural surrogates*, that can learn this update from data, rather than an analytical derivation, and be quickly queried [3, 4]. This field of neural surrogates is highly diverse and is rapidly growing, with numerous surrogates proposed based on graph neural networks (GNNs) [5, 6], transformers [7, 8], or convolutional neural networks (CNNs) [9, 10]. In addition to advancements in neural network architectures, many works have aimed to improve different aspects of neural surrogates, such as improving prediction accuracies [11], adapting to irregularly discretized data [12, 13], and scaling models across different datasets [14–17]. The relevant literature is too vast to detail here; however, for a list of representative neural surrogate works and their numerical baselines, we recommend McGreivy and Hakim [18] and for a survey on neural surrogates and operator learning we recommend Kovachki et al. [19].

Contributions. Neural surrogates often treat solution updates as a black box and directly predict the next state, which we call *state prediction* ($\mathbf{u}(t_{n+1}) = F_\theta(\mathbf{u}(t_n))$). State prediction has become the dominant framework for training and querying neural surrogates, as it is the most obvious way to step forward in time, is easy to implement, and allows neural surrogates to take larger steps Δt . However, we believe that this can be an over-simplification and, inspired by numerical methods, we ask if predicting the temporal derivative or *derivative prediction* ($\frac{\partial \mathbf{u}}{\partial t}|_{t=t_n} = F_\theta(\mathbf{u}(t_n))$) can improve neural surrogate accuracies. Importantly, derivative prediction changes the training objective and inference procedure, and this new framework does not contribute additional training cost but can introduce additional inference costs. Fortunately, this is the only practical difference between the two frameworks, allowing derivative prediction to be used with any neural surrogate architecture and generally applied to the same range of PDEs, discretizations, and problem setups.

One may ask why it is necessary to investigate alternative neural surrogate training and inference frameworks. We illustrate its differences in Figure 1 and describe its potential benefits here. Our hypothesis is that the main benefit of derivative prediction is that it allows the use of an ODE integrator to evolve the solution based on the predicted temporal derivative, which can be quickly queried at inference time. This effectively

decouples the prediction problem, where the model learns the spatial dynamics that create the change in solution values, and the numerical integrator forwards the solution in time based on this learned derivative. In many PDE setups, this can greatly simplify the learning objective; rather than needing to collapse a spatial and temporal update under a single model prediction (state prediction), models can focus on learning just the change in solution values, which tend to be more important than the actual value of the solutions. Through experimentation, we show that this can result in more accurate model predictions.

Secondly, derivative prediction can be more flexible during inference than state prediction. State prediction fixes the temporal resolution of the solution to the dataset resolution, whereas derivative prediction can generate solutions of arbitrary temporal resolutions by modifying Δt in the ODE integrator during inference, which could additionally introduce adaptive step sizing for neural surrogates. Furthermore, derivative prediction can take advantage of different integration schemes, such as multi-step, predictor-corrector, or Runge-Kutta methods to improve or adjust solutions during inference. Importantly, under derivative prediction, these modifications during inference do not require re-training the model. We present experimental results demonstrating these additional capabilities.

A subtle but interesting consequence of this is that models trained with derivative prediction can use PDE data more effectively than training in the conventional state prediction framework. A common practice when training neural surrogates is to down-sample PDE data in time, which is usually finely discretized due to numerical solver constraints, and often up to factors of 10^2 - 10^4 . This is necessary since predicting the next timestep directly implicitly fixes the temporal resolution of the learned model; training on the full-resolution data would require models to auto-regressively predict a large number of timesteps due to its fine resolution and therefore quickly accumulate error. Unfortunately, downsampling by large factors results in discarding a considerable amount of PDE data, but since derivative prediction does not fix the model to a temporal resolution, this can be avoided. In particular, models can be trained on the full-resolution data to obtain highly accurate estimates of the instantaneous derivative, which can be used to take variable steps in time when numerically integrating during inference. We provide results demonstrating this as well.

The benefits of the derivative prediction are not without drawbacks. The main limitation of derivative prediction is that it reintroduces numerical error and discretization constraints back into the neural surrogate framework. Specifically, even with perfect estimates of the instantaneous derivative, numerical integrators can still accumulate error over time with large timesteps Δt or chaotic PDE dynamics. While this is an issue, we find that in practice, this additional numerical error is very small when compared to model error, especially when using higher-order integrators. Additionally, common timescales that conventional neural surrogates are trained on are generally small enough for ODE integrators to handle, however this is not always the case. This can be seen for steady-state problems where neural surrogates are tasked with predicting a future steady-state solution given solely the initial condition (such as Darcy Flow); derivative prediction will completely fail since the initial derivative has little correlation to the steady-state solution. While we only consider time-dependent PDEs, we seek to understand the limits of neural surrogates when predicting different timescales, both under state prediction and derivative prediction frameworks. In particular, it is known that neural surrogates can take timesteps that are numerically unstable (e.g., $CFL > 1$), but we seek to understand to what extent this is possible. Lastly, we release the code and datasets for this work here: https://github.com/anthonyzhou-1/temporal_pdes.

2 Related Work

While there exists substantial prior work on using neural surrogates to model PDE solutions, our work’s main contribution is proposing a method to improve solution accuracy that is agnostic to the PDE or surrogate architecture, as well as investigating an alternate training/inference framework. As such, we focus on related works that either propose surrogate-agnostic methods to improve prediction accuracies or use an alternate framework than state prediction in the model design.

Neural Surrogate Modifications. Initial work on neural surrogates designed various architectures to quickly and accurately approximate PDE solutions, including DeepONet [4], neural operators [3], and physics-informed methods [20]. Although powerful on their own, subsequent works have proposed modifications to these architectures to improve accuracy [21–24], generalize to different problems [8, 14], or adapt to complex PDE systems [25–27]. While these modifications are insightful and perform well, they are generally problem-

or model-specific, which limits their applicability. To address this, prior work has also considered proposing training modifications or guidelines to improve surrogate accuracies [16]. One such example is the use of data augmentations to improve neural surrogate training and prediction accuracy [28]. In addition, previous work has explored the idea of noising data or unrolled training to improve neural surrogate stability and robustness [12, 14, 29]. Lastly, an interesting set of works seek to train refiner modules alongside neural surrogates to improve solution accuracy [11].

Residual Prediction. Prior work has also examined learning physics under different training and prediction frameworks. Besides state prediction, the most common training framework is to predict the residual between the input and the target, or *residual prediction*. Residual prediction can be seen as a special case of derivative prediction, where the residual is a scaled forward Euler approximation of the temporal derivative; however, the temporal resolution is still fixed during inference. Despite residual prediction being used widely in weather applications [30, 31], its use in PDE applications can only be found in certain models [27, 32–35], with its adoption on an ad hoc basis. Therefore, this paper seeks to understand the benefits/drawbacks of different prediction frameworks to better motivate residual prediction and more broadly, derivative prediction.

Hybrid Solvers. Another set of more restrictive, but more targeted training frameworks is to use the neural surrogate to approximate quantities within a conventional solver, creating a *hybrid solver*. For example, when considering the Navier-Stokes equations, hybrid solvers can use a neural surrogate to approximate the convective flux due to its large computational burden and solve the remaining terms or steps numerically [36, 37]. For other equations, spatial derivatives can also be individually approximated using a neural surrogate [38], and more generally, neural surrogates have found use in approximating costly terms within numerical solvers using data [39, 40]. While these frameworks also simplify the training objective by focusing on a single phenomena to model, they are tied to a specific problem or numerical solver.

Neural Network Frameworks. While this paper considers time-dependent PDE modeling, broader interest in neural network prediction frameworks in the machine learning community has also proposed related training and inference procedures. Neural ODEs [41] also predict derivatives, however these are with respect to the network’s hidden state and are not used to predict physical quantities such as in derivative prediction. Additionally, this introduces significant training difficulties [42] which are not present in derivative prediction since the target is not a derivative with respect to the model parameters. If we consider the PDE to be solved under Hamiltonian or Lagrangian mechanics, we can construct a neural network to predict the Hamiltonian or Lagrangian, which can be subsequently integrated to recover physical quantities continuously in time [43–45]. Although interesting, these Hamiltonian or Lagrangian neural networks have seen little adoption to solve PDE problems largely because many PDE systems cannot be conveniently formulated with a Hamiltonian or Lagrangian, and using the approximated Hamiltonian or Lagrangian to evolve physical quantities is computationally expensive. Lastly, solving PDEs under Newtonian mechanics is more mature, with most numerical solvers and neural surrogates being developed under a Newtonian framework.

3 Methods

3.1 Training

During training, models parameterized by F_θ are given the current solution $\mathbf{u}(t_n)$ and timestep t_n , and are trained to predict either $\mathbf{u}(t_{n+1})$ (state prediction) or $\frac{\partial \mathbf{u}}{\partial t}|_{t=t_n}$ (derivative prediction). From a deep learning perspective, this does not change the model, architecture, or training procedure, aside from the need to compute temporal derivatives from the dataset to use as labels. This can be done numerically, such as with a forward Euler scheme ($\frac{\mathbf{u}(t_{n+1}) - \mathbf{u}(t_n)}{\Delta t}$), central difference scheme ($\frac{\mathbf{u}(t_{n+1}) - \mathbf{u}(t_{n-1})}{2\Delta t}$), or higher-order Richardson extrapolations. Additionally, at the endpoints of the dataset a one-sided Richardson extrapolation can be used to obtain accurate estimates of the temporal derivative [46]. By using increasingly higher-order finite-difference schemes, training labels can be made increasingly accurate as well. Additionally, the current time is passed into the model through using Fourier features [47] to project the timestep t_n to a higher dimension and using Adaptive Layer Normalization. Lastly, depending on the PDE setup, coefficient information can also be provided to the model in a similar manner.

3.2 Inference

Once trained to produce accurate estimates of $F_\theta(\mathbf{u}(t_n), t_n) \approx \frac{\partial \mathbf{u}}{\partial t}|_{t=t_n}$, an ODE integrator can be used to evolve the solution forward in time during inference. Specifically, we consider using the Forward Euler, Adams-Bashforth, Heun’s, or 4th-order Runge-Kutta (RK4) method. The update rules are given below:

$$\mathbf{u}(t_{n+1}) = \mathbf{u}(t_n) + \Delta t F_\theta(\mathbf{u}(t_n), t_n) \quad (\text{Forward Euler})$$

$$\mathbf{u}(t_{n+1}) = \mathbf{u}(t_n) + \frac{3\Delta t}{2} F_\theta(\mathbf{u}(t_n), t_n) - \frac{\Delta t}{2} F_\theta(\mathbf{u}(t_{n-1}), t_{n-1}) \quad (\text{Adams-Bashforth})$$

$$\begin{aligned} \tilde{\mathbf{u}}(t_{n+1}) &= \mathbf{u}(t_n) + \Delta t F_\theta(\mathbf{u}(t_n), t_n) \\ \mathbf{u}(t_{n+1}) &= \mathbf{u}(t_n) + \frac{\Delta t}{2} (F_\theta(\mathbf{u}(t_n), t_n) + F_\theta(\tilde{\mathbf{u}}(t_{n+1}), t_{n+1})) \end{aligned} \quad (\text{Heun’s Method})$$

$$\begin{aligned} k_1 &= F_\theta(\mathbf{u}(t_n), t_n) \\ k_2 &= F_\theta(\mathbf{u}(t_n) + \Delta t \frac{k_1}{2}, t_n + \frac{\Delta t}{2}) \\ k_3 &= F_\theta(\mathbf{u}(t_n) + \Delta t \frac{k_2}{2}, t_n + \frac{\Delta t}{2}) \\ k_4 &= F_\theta(\mathbf{u}(t_n) + \Delta t k_3, t_n + \Delta t) \\ \mathbf{u}(t_{n+1}) &= \mathbf{u}(t_n) + \frac{\Delta t}{6} (k_1 + 2k_2 + 2k_3 + k_4) \end{aligned} \quad (\text{4th-order Runge-Kutta})$$

When using the Forward Euler or Adams-Bashforth methods during inference, the computational cost is the same as state prediction, due to only needing to evaluate the model once per timestep. In fact, for explicit multistep methods (such as Adams-Bashforth), previous derivative estimates $F_\theta(\mathbf{u}(t_{n-s}), t_{n-s})$ can be cached during inference to take more accurate forward steps without extra computational cost. However, if using Heun’s or the RK4 method, the computational cost during inference is doubled or quadrupled, due to needing additional derivative estimates to evolve the solution forward in time. While more computationally expensive, this is a worthwhile tradeoff in conventional numerical schemes, as the higher accuracy of higher-order methods facilitates substantially larger timesteps Δt , which reduces the solution time overall even when considering the additional cost of solving a single timestep. Interestingly, we show that this observation can still be true in neural surrogate settings. Lastly, the additional overhead of performing numerical integration during inference is negligible with respect to the forward pass of the model; indeed, within numerical schemes, the temporal update is usually very fast with respect to other operations.

3.3 Equations Considered

1D PDEs. To evaluate the proposed method, we consider testing on a wide range of PDE equations and setups. In 1D we consider the Advection, Heat, and Kuramoto-Sivashinsky (KS) equations:

$$\partial_t u + c \partial_x u = 0 \quad (\text{Adv})$$

$$\partial_t u - \nu \partial_{xx} u = 0 \quad (\text{Heat})$$

$$\partial_t u + u \partial_x u + \partial_{xx} u + \partial_{xxxx} u = 0 \quad (\text{KS})$$

For all 1D equations, initial conditions are generated from a random sum of sines:

$$u(0) = \sum_{j=1}^J A_j \sin(2\pi l_j x / L + \phi_j), \quad (2)$$

where we uniformly sample $A_j \in [-0.5, 0.5]$, $\omega_j \in [-0.4, 0.4]$, $l_j \in \{1, 2, 3\}$, $\phi_j \in [0, 2\pi)$ while fixing $J = 5$, $L = 16$. Samples are generated at a spatial resolution of $n_x = 100$ on a domain $x \in [0, 16]$. The Advection and Heat equations are solved from $t = 0$ to $t = 2$, while the KS equations are solved from $t = 0$ to $t = 100$ due to the different dynamics. Additionally equations coefficients are uniformly sampled for the Advection and Heat equations to introduce additional difficulty: $c \in [0.1, 2.5]$, $\nu \in [0.1, 0.8]$. For the KS equation, coefficients are kept fixed to the more challenging dynamics. Periodic boundary conditions are used for all equations. Lastly, 4096 training samples and 256 validation samples are used for all PDEs.

While conventionally a minor detail, we find that care must be taken when choosing the temporal discretization of the dataset. In state prediction, the temporal resolution must be fine enough to resolve important dynamics, yet not too fine to introduce excessive error propagation during inference. For many PDEs, such as turbulence, this can be a compromise where one objective cannot be improved without sacrificing the other [48]. In the context of derivative prediction, the temporal discretization is less restrictive since the model is not constrained to a resolution defined by the dataset. However, during inference, the timestep cannot be excessively large as to introduce error from the ODE integrator and shift the input distribution to the model. For the main experiments, the discretization is chosen to be 125 timesteps ($\Delta t = 0.016s$) for the Advection and Heat equations, and 400 timesteps ($\Delta t = 0.25$) for the KS equation, although these will be varied when investigating the effect of varying timescales on neural surrogate performance.

2D PDEs. In 2D we consider the Burgers’ and Navier-Stokes (NS) equations:

$$\begin{aligned} \partial_t u + u(\mathbf{c} \cdot \nabla u) - \nu \nabla^2 u &= 0 && \text{(Burgers)} \\ \partial_t \omega + u \cdot \nabla \omega - \nu \nabla^2 \omega = f(x), \quad \nabla \cdot u &= 0 && \text{(NS)} \end{aligned}$$

For the Burgers’ equation, initial conditions are generated from a random sum of sines:

$$u(0) = \sum_{j=1}^J A_j \sin(2\pi l_{xj} x/L + 2\pi l_{yj} y/L + \phi_j) \quad (3)$$

Initial condition parameters are uniformly sampled from $A_j \in [-0.5, 0.5]$, $\omega_j \in [-0.4, 0.4]$, $l_{xj} \in \{1, 2, 3\}$, $l_{yj} \in \{1, 2, 3\}$, $\phi_j \in [0, 2\pi)$ while fixing $J = 5$, $L = 2$. The vorticity form is used for the 2D Navier-Stokes equations; the initial conditions are sampled from a Gaussian random field, and the forcing function is fixed according to Li et al. [3]. The Burgers’ equation is solved on a domain $(x, y) = [-1, 1]^2$ from $t = 0$ to $t = 2$, while the Navier-Stokes equation is solved on a domain $(x, y) = [0, 1]^2$ from $t = 0$ to $t = 50$. The spatial resolution of both datasets are the same at 64×64 . The coefficients in the Burgers’ equation are uniformly sampled from $\nu \in [7.5 \times 10^{-3}, 1.5 \times 10^{-2}]$, and $\mathbf{c} = [c_x, c_y] \in [0.5, 1.0]^2$, while the viscosity in the Navier-Stokes equations is set to 1×10^{-3} . For the main experiments, the Burgers’ equation is discretized at 100 timesteps ($\Delta t = 0.02s$) and the Navier-Stokes equations are discretized at 400 timesteps ($\Delta t = 0.125s$); additionally, the first 25% of data for the Navier-Stokes equations (100 timesteps) are discarded to allow flow patterns to develop from the initial random field. Lastly, 1024 training samples and 256 validation samples are used for all equations.

4 Results

4.1 Prediction Accuracy

In all experiments, we consider evaluating the method using a Fourier Neural Operator (FNO) [3] and Unet [10], which are two popular model choices for benchmarking uniform-grid PDE prediction problems [49, 50]. Models are either trained with the state prediction objective (State Pred.), or the derivative prediction objective with a 4-th order Richardson’s extrapolation to ensure the accuracy of the training labels. Furthermore, different integration schemes are evaluated during inference. Models are evaluated on a validation set by computing either the rollout error or correlation time. Rollout error is defined to be the relative L2 error of the predicted, auto-regressive trajectory with respect to the true trajectory, averaged over all timesteps. In chaotic systems such as the KS equation, rollout error can be heavily skewed once model predictions diverge, therefore correlation time is used to judge model performance. Correlation time is defined to be the timestep after which model predictions have a Pearson correlation of less than 0.8 with respect to the ground truth.

| PDE: | Adv | Heat | KS | Burgers | NS |
|--------------------|--------------|--------------|--------------|--------------|--------------|
| Metric: | Roll. Err. ↓ | Roll. Err. ↓ | Corr. Time ↑ | Roll. Err. ↓ | Roll. Err. ↓ |
| FNO (State Pred.) | 0.544 | 0.589 | 140.75 | 0.437 | 0.715 |
| FNO (FwdEuler) | 0.048 | 0.141 | 85.75 | 0.196 | 0.159 |
| FNO (Adams) | 0.032 | 0.141 | 177 | 0.174 | 0.100 |
| FNO (Heun) | 0.032 | 0.141 | 183 | 0.175 | 0.100 |
| FNO (RK4) | 0.033 | 0.141 | 184 | 0.175 | 0.100 |
| Unet (State Pred.) | 0.386 | 0.199 | 70 | Unstable | Unstable |
| Unet (FwdEuler) | 0.125 | 0.141 | 65.75 | 0.444 | 0.384 |
| Unet (Adams) | 0.117 | 0.141 | 79.5 | 0.397 | 0.334 |
| Unet (Heun) | 0.117 | 0.141 | 79.75 | 0.400 | 0.333 |
| Unet (RK4) | 0.116 | 0.141 | 80.25 | 0.402 | 0.333 |

Table 1: Results on prediction accuracy across different PDEs, models, and training/inference frameworks.

Validation metrics are reported in Table 1. We find that derivative prediction can achieve much lower errors than state prediction across equations and model choices. One hypothesized reason for this is because derivative prediction can be more stable than state prediction; both models are trained such that the one-step training error is very low, however, during inference, using state prediction leads to error accumulation and even unstable rollouts. From this point of view, incorporating an ODE integrator during inference can help stabilize neural surrogate predictions by using a numerical, physics-based prior to update the solution.

For equations with simple dynamics, such as the Advection, Heat, and 2D Burgers equations, we observe that using higher-order ODE integrators does not significantly affect accuracies, although the Forward Euler method can perform worse. This doesn’t mean higher-order integrators aren’t useful; they can still accelerate inference times by taking larger timesteps during inference due to being more robust. However, within this experimental setup, the Adams-Bashforth method can be a good choice during inference due to its higher accuracy and identical inference cost to the Forward Euler method or state prediction. For more challenging systems, such as the KS equation, higher-order integrators can be more accurate, since coarser integrators can accumulate larger errors and shift the input distribution during inference. Lastly, we note that the ODE integrator can be changed during inference without re-training the model, allowing the speed or accuracy of models trained with derivative prediction to be easily changed.

Additionally, we plot sample rollouts of FNO and Unet models trained using state prediction or derivative prediction with an RK4 integrator. Results in 1D and 2D are plotted in Figure 2 and Figure 3. Interestingly, FNO models struggle with simple 1D dynamics, which is corroborated by the validation metrics. We believe that this is due to overfitting, where FNO models largely optimize for one-step accuracy without long-term stability. Indeed, when applying pushforward or refiner methods in the following section, the error of FNO methods on simple 1D problems improves drastically. Unet models perform better on the Advection and Heat equations; however, stability is still a challenge, with spurious predictions being made at later timesteps. Applying derivative prediction can fix these issues and lead to stable, accurate predictions for simple 1D PDEs. For more chaotic 1D systems, such as the KS equation, derivative prediction is able to delay error accumulation and extend the correlation time of predictions. Furthermore, derivative prediction can stabilize Unet predictions, despite being inaccurate in the long term.

For 2D systems, derivative prediction can similarly stabilize FNO and Unet predictions. Unet models are especially prone to error propagation, since FNO models have helpful inductive biases that create sinusoidal outputs. Applying derivative prediction can result in accurate solutions; however, for more complex systems (NS), solutions eventually lose accuracy.

As a whole, these results suggest that there can be benefits in learning the temporal derivative, rather than directly predicting the next state, and in practice, implementing this through different ODE integrators can further affect accuracy. Apart from being more stable, we hypothesize that learning a derivative can be beneficial due to decomposing the solution step into a spatial and temporal update; learning just the spatial update and letting an ODE integrator perform the temporal update can be easier than relying on a model to learn both. We empirically validate this in Figure 5, but leave further analysis to the discussion section.

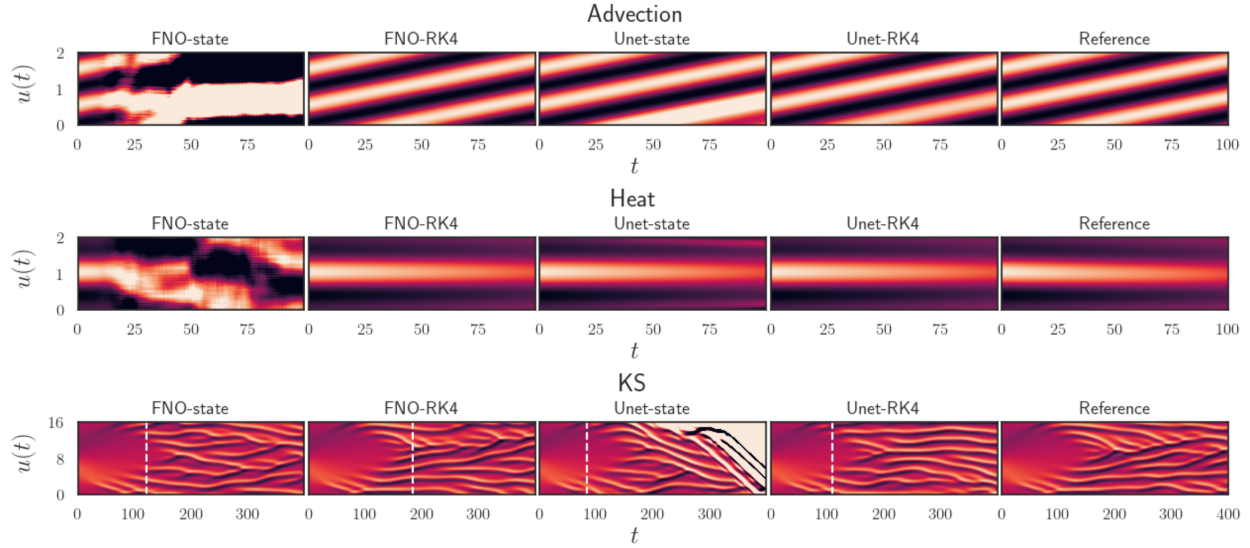


Fig. 2: Comparison of state prediction and derivative prediction using an RK4 integrator on 1D PDEs. Time is plotted on the x-axis and nodal values on the y-axis. Correlation time is denoted for the KS equation.

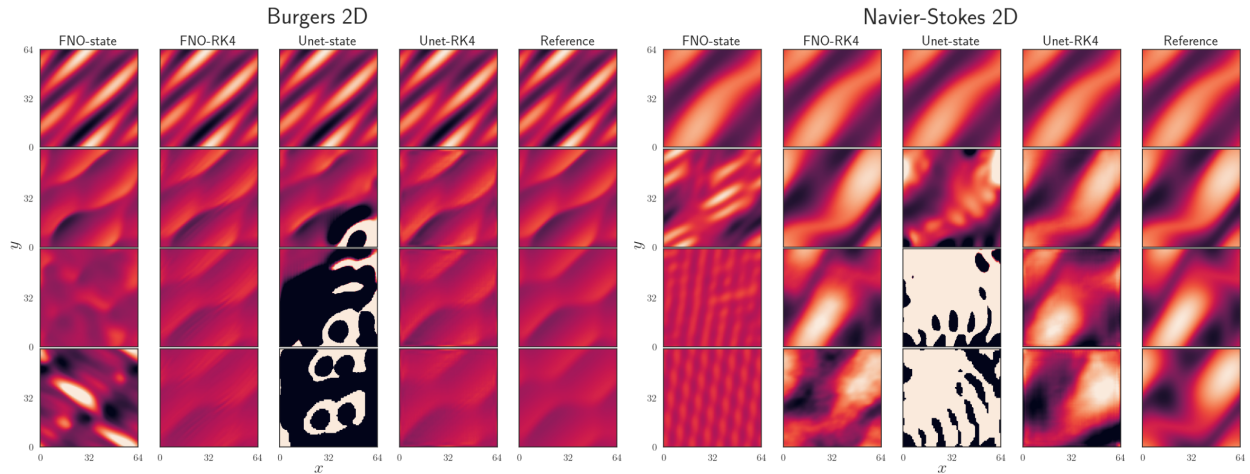


Fig. 3: Comparison of state prediction and derivative prediction using an RK4 integrator on 2D PDEs. The spatial dimensions are plotted for each frame, at multiple snapshots in time from top to bottom.

4.2 Comparison to Training Modifiers

We compare our approach with various methods to improve the prediction accuracy of models, including using 4 times as many model parameters, implementing the pushforward trick/unrolled training [12, 29], or using the PDE-Refiner framework [11]. The pushforward trick, or unrolled training, aims to improve rollout stability and accuracy by introducing model noise during training. This is done by making a model prediction $\hat{\mathbf{u}}$, then using this model prediction as an input to make another prediction $F_\theta(\hat{\mathbf{u}})$, which is compared to the ground truth to evaluate a loss. This unrolling can also be done for multiple timesteps, however, the compute and memory scales linearly with each additional unrolled timestep. Additionally, the gradient can be calculated with respect to only the final timestep or all timesteps (non-differentiable/differentiable unrolling). For our implementation, we follow Brandstetter et al. [12] and unroll the training for 1 additional timestep while letting this unrolling be non-differentiable. Furthermore, we allow the model to train without the pushforward trick for a certain number of initial epochs to prevent excessive model noise from degrading its training.

| PDE: | Adv | Heat | KS | Burgers | NS |
|--------------------|--------------|--------------|--------------|--------------|--------------|
| Metric: | Roll. Err. ↓ | Roll. Err. ↓ | Corr. Time ↑ | Roll. Err. ↓ | Roll. Err. ↓ |
| FNO (State Pred.) | 0.544 | 0.589 | 140.75 | 0.437 | 0.715 |
| FNO (4x params) | 0.826 | 0.991 | 156.25 | 0.276 | 0.599 |
| FNO (Pushforward) | 0.357 | 0.486 | 146 | 0.397 | 0.090 |
| FNO (Refiner) | 0.036 | 0.167 | 148.75 | 1.141 | 0.596 |
| FNO (RK4) | 0.033 | 0.141 | 184 | 0.175 | 0.100 |
| Unet (State Pred.) | 0.386 | 0.199 | 70 | Unstable | Unstable |
| Unet (4x params) | 0.370 | 0.147 | 67.25 | Unstable | 0.457 |
| Unet (Pushforward) | 0.276 | 0.169 | 76.75 | Unstable | Unstable |
| Unet (Refiner) | 0.275 | 0.175 | 63.5 | 0.313 | 0.235 |
| Unet (RK4) | 0.116 | 0.141 | 80.25 | 0.402 | 0.333 |

Table 2: Comparing different training modifications on various PDEs and models.

While unrolled training is a simple and often effective method to improve neural surrogate accuracy, further gains in accuracy have been demonstrated by using a probabilistic refinement of predicted solutions to better recover the true solution spectrum, which we call refiner methods [11, 51]. These methods work by adding Gaussian noise to the prediction target and training a refinement model to denoise this input to match the target. While the specific implementation can vary, these methods generally sample random noise during inference and, conditioned on a past timestep, take several refinement steps to produce a future solution. For our benchmark, we follow Lippe et al. [11] and use three refinement steps.

We train models using various modifications with the state prediction framework and additionally report baseline models using only state prediction and derivative prediction with an RK4 integrator. Validation metrics are reported in Table 2. We reproduce previous results showing the effectiveness of scaling model size, unrolled training, and refiner methods, which tend to improve the performance of neural surrogates across many PDEs and models. However, we observe the improvement of these modifications can be more nuanced. For example, scaling the model size can depend on the architecture’s scalability and capacity, as well as data constraints to prevent overfitting. Indeed, we observe that FNO models tend to overfit in simple test cases (Advection, Heat), while Unet models do not, underlining previous results on the scalability of Unet vs. FNO models in PDE contexts [16]. Furthermore, while refiner methods are very powerful, in some cases achieving the best performance, introducing a denoising objective creates additional complexity during training, and in rare cases performs worse than a baseline. Refiner methods can also be dependent on model architecture, with some models performing better than others on denoising; in particular, FNO models can struggle with spurious high frequencies introduced by Gaussian noise that are exacerbated in 2D PDEs.

Lastly, using the pushforward trick tends to consistently improve model performance, likely due to the simplicity of the method in improving robustness to model noise. Likewise, the simplicity of using a different training objective in derivative prediction also leads to consistent improvements in model performance, outperforming unrolled training and suggesting that derivative prediction can be generally applicable across different architectures and problems. In addition, derivative prediction does not add additional training cost, while other training modifications generally require more compute and memory.

It is also interesting to note that these modifications are not exclusive of each other; in fact, it is straightforward to implement derivative prediction in conjunction with scaling the model size, using unrolled training, or applying refiner methods to further improve performance. As a final remark, while overall performance gains of these methods support prior work and observations, applying these training modifications successfully still requires an understanding of the problem setup, model capacity, dataset size, or relevant theory, as the results show that training intricacies and exceptions to overall trends still exist. Much like any numerical or machine-learning method, using derivative prediction similarly has these caveats, however, we leave this discussion to later sections.

4.3 Inference Modifications

A potential benefit of derivative prediction is its flexibility: predicting temporal derivatives allows the temporal resolution of the model to not be fixed. This can be taken advantage of to train on more data, not in

| PDE: Metric: | Adv Roll. Err. ↓ | NS Roll. Err. ↓ | PDE: Metric: | Adv Roll. Err. ↓ | NS Roll. Err. ↓ |
|---------------------------|---------------------|--------------------|----------------------------|---------------------|--------------------|
| FNO (FwdEuler) | 0.048 | 0.159 | Unet (FwdEuler) | 0.125 | 0.384 |
| FNO (FwdEuler + 2x data) | 0.045 | 0.139 | Unet (FwdEuler + 2x data) | 0.119 | 0.345 |
| FNO (FwdEuler + 2x steps) | 0.037 | 0.120 | Unet (FwdEuler + 2x steps) | 0.120 | 0.346 |
| FNO (Heun) | 0.033 | 0.100 | Unet (Heun) | 0.117 | 0.333 |

Table 3: Comparing different inference modifications across various models and PDEs.

the sense of generating more data samples but using more of the existing data at a finer temporal discretization. In fact, PDE data are usually heavily downsampled in time to prevent models that use state prediction from being fixed to a fine temporal resolution, yet this discards a large proportion of the generated data. We test if using more data is beneficial by training a model using derivative prediction on data discretized at half the temporal resolution (2x data). For our test cases, this results in using 250 timesteps instead of 125 timesteps for Adv/Heat and 600 timesteps instead of 300 timesteps for NS, while keeping the start and end time of the trajectories the same. During inference, models still make predictions at the native resolution, after being trained on twice the data at the finer resolution.

Alternatively, since the temporal resolution is not fixed, during inference the ODE integrator can take smaller steps in time to potentially improve neural surrogate accuracies. We test whether taking more steps is beneficial by training a model at the native resolution, but taking twice as many steps (2x steps) during inference. This amounts to setting Δt to half its original size in the ODE integrator. Additionally, predictions at half-steps are discarded, and rollout errors are calculated at the native resolution.

We report the results of training on more finely discretized data (2x data) and taking smaller timesteps during inference (2x steps) in Table 3. Results are evaluated for the Advection and Navier-Stokes equations to validate these ideas on a simple 1D case and a more complex 2D case. In addition, we also report baselines using the Forward Euler or Heun’s method without modifications. Interestingly, training on more finely discretized data can result in lower rollout errors without additional inference cost, likely from learning more accurate derivative estimates. This effect is also more apparent in more complex systems (NS), where more data and better derivative estimates become more important. This opens opportunities for models trained using derivative prediction to discard less data than conventional state prediction frameworks and achieve better performance. However, we hypothesize this can have diminishing returns, as further increasing the resolution of the dataset results in adding data samples that are already very similar to the existing dataset.

Furthermore, taking smaller steps during inference can also decrease rollout error, but at the cost of more compute. Interestingly, taking more steps does not result in higher error propagation; despite rolling out trajectories to twice the original length (even up to 600 steps in NS), the error remains stable and even decreases when the trajectory length increases. This is opposite to conventional observations when training models using state prediction, where rollout error increases as more steps are taken during inference [11, 12, 48]. Again, we hypothesize that this stability is due to using a numerical integrator to evolve forward in time, rather than relying on the model to do so.

However, we note that lower errors can also be achieved by using higher-order integrators rather than smaller steps. Indeed, Heun’s method adds a corrector step to the Forward Euler method to achieve a higher-order approximation, but uses twice the compute. Therefore, while the computational cost of using Heun’s method and the Forward Euler method with half the step size is equal, using Heun’s method during inference is still more accurate. A consequence of this is that if speed is preferred during inference, using higher-order schemes with a larger step size could still outperform lower-order schemes with smaller step sizes, despite the additional compute of higher-order schemes. Alternatively, in cases where additional accuracy is important, higher-order integrators can also be used with smaller step sizes to improve accuracy. Indeed, one of the main benefits of derivative prediction is being able to adaptively change the step size during inference, which can lead to taking larger steps where the solution changes slowly and smaller steps where the solution changes quickly.

4.4 Prediction Timescales

The main limitation of derivative prediction is that it reintroduces discretization constraints and numerical error to neural surrogates. To evaluate the extent of this limitation, we consider training models

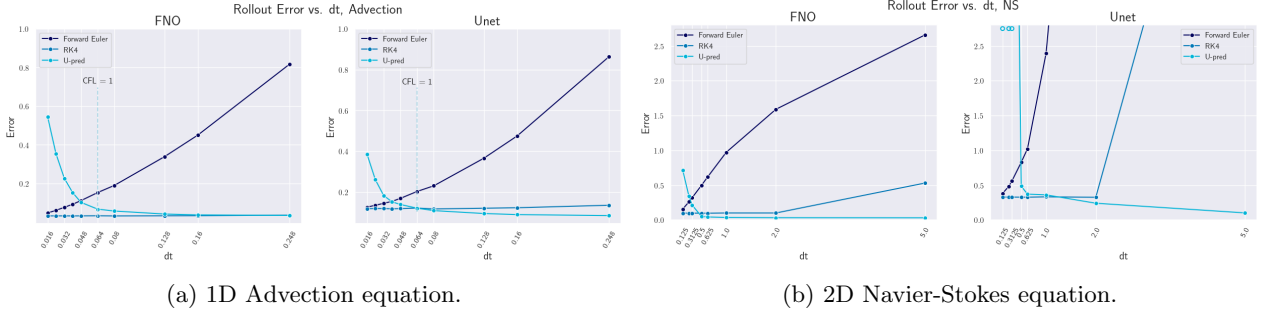


Fig. 4: Rollout error of FNO or Unet models trained with state prediction or derivative prediction with a Forward Euler or RK4 integrator; errors are plotted after predicting solutions at different timescales Δt . The resolution where $CFL = 1$ is denoted for 1D Advection. Empty circles denote unstable rollouts.

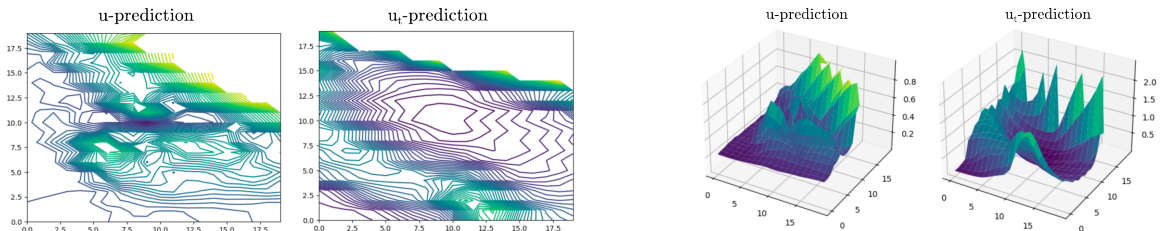
using state prediction at different temporal resolutions, as well as evaluating a model trained using derivative prediction at different step sizes Δt . This is done for both FNO and Unet models, and with the 1D Advection and 2D Navier-Stokes equations. For 1D Advection, the different timescales considered are: $\Delta t = 0.016, 0.024, 0.032, 0.04, 0.048, 0.064, 0.08, 0.128, 0.160, 0.248$ seconds, corresponding to predicting 125, 80, 60, 50, 40, 30, 25, 15, 12 or 8 steps of the solution trajectory. For the 2D Navier-Stokes equations, the different timescales considered are: $\Delta t = 0.125, 0.25, 0.3125, 0.5, 0.625, 1.0, 2.0, 5.0$ seconds, corresponding to predicting 400, 200, 150, 100, 75, 50, 25, or 10 steps of the solution trajectory. One remark is that models using state prediction need to be re-trained for each resolution, while a single model trained using derivative prediction can be queried at these resolutions during inference.

The results of this evaluation are plotted in Figure 4. We observe that as Δt increases during inference, models trained with derivative prediction tend to have higher errors due to accumulating error from numerical integration. Using higher-order schemes, such as RK4, alleviates this problem, but for more complex systems (NS) the step size can eventually become too large. We observe that the opposite trend is true for models trained with state prediction. In fact, it is well known that the rollout error of models decreases as the trajectory length decreases (i.e., Δt increases), due to lower error propagation and the ability for neural surrogates to circumvent conventional step sizing constraints.

Indeed, for the 1D Advection equation, models trained with state prediction remain stable in regimes where the CFL number ($\frac{c\Delta t}{\Delta x}$) is well above 1. Interestingly, this is also true for models trained with derivative prediction if a suitable integrator is used during inference. For the 2D Navier-Stokes equations, a similar stability criterion does not exist, however a very coarse criterion can be estimated by considering the stability of just the viscous term $\nu \nabla^2 \mathbf{u}$. This viscous term is stable when $\Delta t \leq \frac{(\Delta x)^2}{2\nu} \approx 0.122s$, which gives an upper bound to the step sizing; in reality, non-linear terms in the Navier-Stokes equations will likely necessitate a much smaller step size. Therefore, all timescales considered for the Navier-Stokes equations are numerically unstable, yet models trained with both state prediction and derivative prediction can still be accurate, albeit with different exceptions. State prediction can be unstable at small Δt due to auto-regressive error accumulation and derivative prediction can be unstable at large Δt due to error from numerical integration.

Given these limitations of derivative prediction it is worth addressing to what extent this is an issue. Despite including a numerical integrator, derivative prediction can still be stable in highly numerically unstable regimes due to having data-driven derivative estimates. However, at very large Δt this is no longer true; however, predictions with such coarse temporal resolution may not even be useful. In fact, when taking only 10 steps for the Navier-Stokes equations ($\Delta t = 5s$) the predicted frames are so distinct that meaningful dynamics cannot be reconstructed from these distant frames. Compared to state prediction, using derivative prediction can require taking more steps during inference to maintain stability, however, this can still be fewer steps than a numerical solver. For example, the pseudo-spectral method used to solve the Navier-Stokes equations uses $\Delta t = 1 \times 10^{-4}s$, which corresponds to taking 500,000 steps; with more optimization this can be solved at a coarser resolution, however, derivative prediction will likely still use fewer steps.

5 Discussion



(a) Loss contours of state prediction (left) and derivative prediction (right) (b) Loss surfaces of state prediction (left) and derivative prediction (right)

Fig. 5: Visualization of the loss landscape of state prediction and derivative prediction after training a Unet on 1D Advection. We find that the derivative prediction objective can be empirically easier to learn.

5.1 Loss Landscapes

To understand why derivative prediction may outperform state prediction, we train a Unet on the 1D Advection benchmark using both state and derivative prediction, and visualize the loss landscape using filter normalization [52] in Figure 5. The loss landscape is constructed by perturbing trained weights in a set of normalized, random directions and evaluating the perturbed rollout loss on validation samples. We find that the derivative prediction objective can be empirically easier to learn than the state prediction objective. One potential reason for this is that when solving PDEs at a suitable resolution, future timesteps are often similar to current ones but with slight changes from evolving forward in time. This causes the prediction label to contain redundant information about the current state, where the learning signal comes from the change in state, which can be small. This can contribute to many local minima, where models can learn variations of the identity map that predict potential states that resemble the ground truth, since the forward evolution only slightly changes the solution [27]. However, despite nodal values being similar among local minima, the temporal derivatives at these potential states can be very different. Therefore, derivative prediction can isolate the important dynamics to better distinguish between potential model predictions.

One way to visualize this phenomena is to compare ground-truth and noised PDE data and their derivatives. This is plotted in Figure 6. A ground-truth trajectory \mathbf{u} at a given time t is plotted along with the derivative evaluated at that time $\frac{\partial}{\partial t}(\mathbf{u})$. A small amount of Gaussian noise ($\mathcal{N}(0, 0.01)$), which is centered at $\mu = 0$ and with variance $\sigma^2 = 0.01$, is added to \mathbf{u} at all timesteps, and the derivative is evaluated with respect to this noised trajectory; these quantities are also plotted at the given time t . We make a similar observation: many local minima can be similar to the true state, and indeed adding a small amount of Gaussian noise nearly resembles the true label; however, when taking a temporal derivative, differences between local minima and the true label are highlighted to help models learn the true solution.

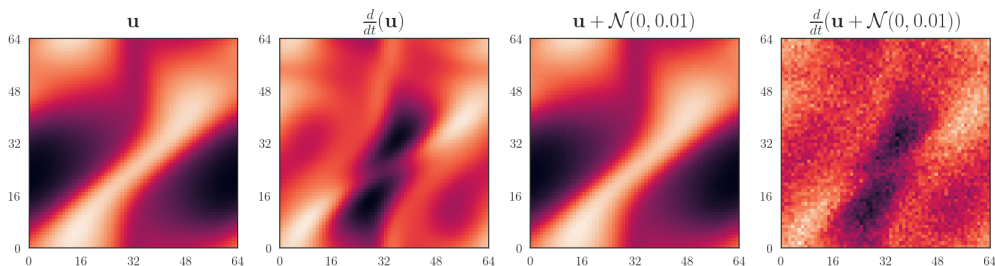


Fig. 6: Snapshots of the 2D Navier-Stokes equation, along with their temporal derivatives. Adding noise to a trajectory creates a similar sample, however this effect is noticeable when taking its temporal derivative.

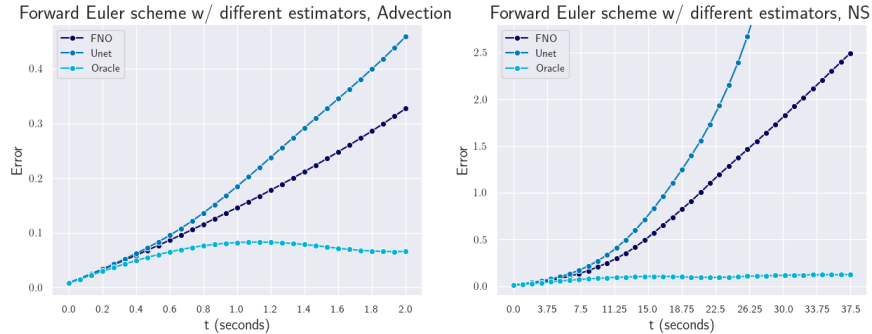


Fig. 7: Error at each timestep using FNO, Unet, or an oracle to estimate $\frac{\partial \mathbf{u}}{\partial t}$ and integrating with the Forward Euler method, for the 1D Advection and 2D NS equations. Each marker denotes an integration step.

5.2 Numerical Error

We have previously shown that numerical error can cause models trained with derivative prediction to become unstable at large Δt , however, we seek to further understand this behavior. In particular, we have access to ground-truth derivative estimates from the ground-truth trajectory; using these estimates rather than neural surrogate estimates can serve as a baseline to compare how much error is being contributed by the ODE integrator. This baseline is called the numerical *oracle*, since it relies on future observations to accurately estimate the instantaneous derivative.

We plot the error over time during inference on the validation set of the 1D Advection and 2D NS equations in Figure 7. The solution is integrated at a sufficiently coarse step size to introduce instability ($\Delta t = 0.064s$ for advection and $\Delta t = 1s$ for NS). The ODE integrator, which in this case is the Forward Euler method, is given derivatives from trained FNO or Unet models, as well as the oracle. We find that despite having near-perfect derivative estimates from the oracle, the integrator still accumulates error over time. However, these errors are still much smaller than querying a neural surrogate for derivative estimates. Therefore, we conclude that the integrator can introduce numerical error, however it is very small with respect to model error, even when considering numerically unstable step sizes. In practice, this means that the model, rather than the framework, is the primary opportunity for improvement.

From training, we know that the one-step training loss is low and can assume that if given a perfect input, models can make an accurate derivative estimate. Indeed, this seems to be the case where the model errors closely follow the oracle errors up to a certain point (around the first 20% of the rollout). However, after this point, the numerical error shifts model inputs such that they no longer match the training distribution, and the model begins to make inaccurate derivative estimates, which contributes model error. Integrating these inaccurate estimates produces model inputs even further from the training distribution, which produces even more inaccurate derivative estimates. This error compounds until the model no longer makes useful predictions.

One avenue to delay this error propagation is to use higher-order schemes to reduce the numerical error and delay the initial shift in model inputs. In fact, this is one reason why higher-order schemes remain more stable at larger time steps as shown in Figure 4. However, reducing model error and improving noise robustness can also delay this error propagation; this opens up promising avenues to apply unrolled training or refiner methods with derivative prediction, which are designed for this purpose.

6 Conclusion

We introduce framing neural surrogates to predict temporal derivatives and use an ODE integrator during inference to produce solutions. Although this idea has been studied informally through residual prediction, this is the first work to formally consider this framework with an ODE integrator and investigate its benefits and limitations. We find that derivative prediction can improve model accuracy and stability across architectures and PDE problems, and has useful data and inference flexibility. Furthermore, we compare this

framework with other training modifications and study the effect of temporal resolution on model performance. Lastly, we hypothesize potential explanations for the improved stability and accuracy of derivative prediction and study the role of numerical error introduced by the ODE integrator. We hope that future work can apply derivative prediction across a wide variety problems and model architectures, and improve performance at coarser step sizes.

7 Declarations

Data availability. Datasets used in this work are provided at: https://huggingface.co/datasets/ayz2/temporal_pdes

Code availability. Code to reproduce this work is provided at: https://github.com/anthonyzhou-1/temporal_pdes

Funding. This research did not receive any specific grant from funding agencies in the public, commercial, or not-for-profit sectors.

References

- [1] Schiesser, W.E.: The Numerical Method of Lines, Integration of Partial Differential Equations. Elsevier (2012)
- [2] Chorin, A.J.: The numerical solution of the navier-stokes equations for an incompressible fluid. Bulletin of the American Mathematical Society (1967)
- [3] Li, Z., Kovachki, N., Azizzadenesheli, K., Liu, B., Bhattacharya, K., Stuart, A., Anandkumar, A.: Fourier Neural Operator for Parametric Partial Differential Equations (2021). <https://arxiv.org/abs/2010.08895>
- [4] Lu, L., Jin, P., Pang, G., Zhang, Z., Karniadakis, G.E.: Learning nonlinear operators via deeponet based on the universal approximation theorem of operators. Nature Machine Intelligence **3**(3), 218–229 (2021) <https://doi.org/10.1038/s42256-021-00302-5>
- [5] Li, Z., Farimani, A.B.: Graph neural network-accelerated lagrangian fluid simulation. Computers & Graphics **103**, 201–211 (2022) <https://doi.org/10.1016/j.cag.2022.02.004>
- [6] Battaglia, P.W., Pascanu, R., Lai, M., Rezende, D., Kavukcuoglu, K.: Interaction Networks for Learning about Objects, Relations and Physics (2016). <https://arxiv.org/abs/1612.00222>
- [7] Li, Z., Meidani, K., Farimani, A.B.: Transformer for Partial Differential Equations’ Operator Learning (2023). <https://arxiv.org/abs/2205.13671>
- [8] Alkin, B., Fürst, A., Schmid, S., Gruber, L., Holzleitner, M., Brandstetter, J.: Universal Physics Transformers: A Framework For Efficiently Scaling Neural Operators (2024). <https://arxiv.org/abs/2402.12365>
- [9] Thuerey, N., Weißenow, K., Prantl, L., Hu, X.: Deep learning methods for reynolds-averaged navier–stokes simulations of airfoil flows. AIAA Journal **58**(1), 25–36 (2020) <https://doi.org/10.2514/1.j058291>
- [10] Gupta, J.K., Brandstetter, J.: Towards Multi-spatiotemporal-scale Generalized PDE Modeling (2022). <https://arxiv.org/abs/2209.15616>
- [11] Lippe, P., Veeling, B.S., Perdikaris, P., Turner, R.E., Brandstetter, J.: PDE-Refiner: Achieving Accurate Long Rollouts with Neural PDE Solvers (2023). <https://arxiv.org/abs/2308.05732>
- [12] Brandstetter, J., Worrall, D., Welling, M.: Message Passing Neural PDE Solvers (2023). <https://arxiv.org/abs/2202.03376>
- [13] Li, Z., Kovachki, N.B., Choy, C., Li, B., Kossaiji, J., Otta, S.P., Nabian, M.A., Stadler, M., Hundt, C., Azizzadenesheli, K., Anandkumar, A.: Geometry-Informed Neural Operator for Large-Scale 3D PDEs (2023). <https://arxiv.org/abs/2309.00583>
- [14] Hao, Z., Su, C., Liu, S., Berner, J., Ying, C., Su, H., Anandkumar, A., Song, J., Zhu, J.: DPOT: Auto-Regressive Denoising Operator Transformer for Large-Scale PDE Pre-Training (2024). <https://arxiv.org/abs/2403.03542>
- [15] Herde, M., Raonić, B., Rohner, T., Käppeli, R., Molinaro, R., Bézenac, E., Mishra, S.: Poseidon: Efficient Foundation Models for PDEs (2024). <https://arxiv.org/abs/2405.19101>
- [16] Zhou, A., Lorsung, C., Hemmasian, A., Farimani, A.B.: Strategies for Pretraining Neural Operators (2024). <https://arxiv.org/abs/2406.08473>
- [17] Zhou, A., Farimani, A.B.: Masked Autoencoders are PDE Learners (2024). <https://arxiv.org/abs/2403.17728>

- [18] McGreivy, N., Hakim, A.: Weak baselines and reporting biases lead to overoptimism in machine learning for fluid-related partial differential equations. *Nature Machine Intelligence* **6**(10), 1256–1269 (2024) <https://doi.org/10.1038/s42256-024-00897-5>
- [19] Kovachki, N., Li, Z., Liu, B., Azizzadenesheli, K., Bhattacharya, K., Stuart, A., Anandkumar, A.: Neural Operator: Learning Maps Between Function Spaces (2024). <https://doi.org/10.5555/3648699.3648788> . <https://arxiv.org/abs/2108.08481>
- [20] Raissi, M., Perdikaris, P., Karniadakis, G.E.: Physics-informed neural networks: A deep learning framework for solving forward and inverse problems involving nonlinear partial differential equations. *Journal of Computational Physics* **378**, 686–707 (2019) <https://doi.org/10.1016/j.jcp.2018.10.045>
- [21] Rahman, M.A., Ross, Z.E., Azizzadenesheli, K.: U-NO: U-shaped Neural Operators (2023). <https://arxiv.org/abs/2204.11127>
- [22] Li, Z., Zheng, H., Kovachki, N., Jin, D., Chen, H., Liu, B., Azizzadenesheli, K., Anandkumar, A.: Physics-Informed Neural Operator for Learning Partial Differential Equations (2023). <https://arxiv.org/abs/2111.03794>
- [23] Wu, H., Luo, H., Wang, H., Wang, J., Long, M.: Transolver: A Fast Transformer Solver for PDEs on General Geometries (2024). <https://arxiv.org/abs/2402.02366>
- [24] Zhou, A., Li, Z., Schneier, M., Jr, J.R.B., Farimani, A.B.: Text2PDE: Latent Diffusion Models for Accessible Physics Simulation (2024). <https://arxiv.org/abs/2410.01153>
- [25] Li, Z., Zhou, A., Patil, S., Farimani, A.B.: CaFA: Global Weather Forecasting with Factorized Attention on Sphere (2024). <https://arxiv.org/abs/2405.07395>
- [26] Pathak, J., Subramanian, S., Harrington, P., Raja, S., Chattopadhyay, A., Mardani, M., Kurth, T., Hall, D., Li, Z., Azizzadenesheli, K., Hassanzadeh, P., Kashinath, K., Anandkumar, A.: FourCastNet: A Global Data-driven High-resolution Weather Model using Adaptive Fourier Neural Operators (2022). <https://arxiv.org/abs/2202.11214>
- [27] Li, Z., Liu-Schiaffini, M., Kovachki, N., Liu, B., Azizzadenesheli, K., Bhattacharya, K., Stuart, A., Anandkumar, A.: Learning Dissipative Dynamics in Chaotic Systems (2022). <https://arxiv.org/abs/2106.06898>
- [28] Brandstetter, J., Welling, M., Worrall, D.E.: Lie point symmetry data augmentation for neural pde solvers. *arXiv preprint arXiv:2202.07643* (2022)
- [29] List, B., Chen, L.-W., Bali, K., Thuerey, N.: Differentiability in unrolled training of neural physics simulators on transient dynamics. *Computer Methods in Applied Mechanics and Engineering* **433**, 117441 (2025) <https://doi.org/10.1016/j.cma.2024.117441>
- [30] Lam, R., Sanchez-Gonzalez, A., Willson, M., Wirnsberger, P., Fortunato, M., Alet, F., Ravuri, S., Ewalds, T., Eaton-Rosen, Z., Hu, W., Merose, A., Hoyer, S., Holland, G., Vinyals, O., Stott, J., Pritzel, A., Mohamed, S., Battaglia, P.: GraphCast: Learning skillful medium-range global weather forecasting (2023). <https://arxiv.org/abs/2212.12794>
- [31] Price, I., Sanchez-Gonzalez, A., Alet, F., Andersson, T.R., El-Kadi, A., Masters, D., Ewalds, T., Stott, J., Mohamed, S., Battaglia, P., Lam, R., Willson, M.: GenCast: Diffusion-based ensemble forecasting for medium-range weather (2024). <https://arxiv.org/abs/2312.15796>
- [32] Pfaff, T., Fortunato, M., Sanchez-Gonzalez, A., Battaglia, P.W.: Learning Mesh-Based Simulation with Graph Networks (2021). <https://arxiv.org/abs/2010.03409>

- [33] Stachenfeld, K., Fielding, D.B., Kochkov, D., Cranmer, M., Pfaff, T., Godwin, J., Cui, C., Ho, S., Battaglia, P., Sanchez-Gonzalez, A.: Learned Coarse Models for Efficient Turbulence Simulation (2022). <https://arxiv.org/abs/2112.15275>
- [34] Sanchez-Gonzalez, A., Godwin, J., Pfaff, T., Ying, R., Leskovec, J., Battaglia, P.W.: Learning to Simulate Complex Physics with Graph Networks (2020). <https://arxiv.org/abs/2002.09405>
- [35] Wang, R., Kashinath, K., Mustafa, M., Albert, A., Yu, R.: Towards Physics-informed Deep Learning for Turbulent Flow Prediction (2020). <https://arxiv.org/abs/1911.08655>
- [36] Kochkov, D., Smith, J.A., Alieva, A., Wang, Q., Brenner, M.P., Hoyer, S.: Machine learning–accelerated computational fluid dynamics. *Proceedings of the National Academy of Sciences* **118**(21), 2101784118 (2021) <https://doi.org/10.1073/pnas.2101784118> <https://www.pnas.org/doi/pdf/10.1073/pnas.2101784118>
- [37] Sun, Z., Yang, Y., Yoo, S.: A neural pde solver with temporal stencil modeling (2023)
- [38] Bar-Sinai, Y., Hoyer, S., Hickey, J., Brenner, M.P.: Learning data-driven discretizations for partial differential equations. *Proceedings of the National Academy of Sciences* **116**(31), 15344–15349 (2019) <https://doi.org/10.1073/pnas.1814058116> <https://www.pnas.org/doi/pdf/10.1073/pnas.1814058116>
- [39] Margenberg, N., Jendersie, R., Lessig, C., Richter, T.: Dnn-mg: A hybrid neural network/finite element method with applications to 3d simulations of the navier–stokes equations. *Computer Methods in Applied Mechanics and Engineering* **420**, 116692 (2024) <https://doi.org/10.1016/j.cma.2023.116692>
- [40] Liu, B., Kovachki, N., Li, Z., Azizzadenesheli, K., Anandkumar, A., Stuart, A.M., Bhattacharya, K.: A learning-based multiscale method and its application to inelastic impact problems. *Journal of the Mechanics and Physics of Solids* **158**, 104668 (2022) <https://doi.org/10.1016/j.jmps.2021.104668>
- [41] Chen, R.T.Q., Rubanova, Y., Bettencourt, J., Duvenaud, D.: Neural Ordinary Differential Equations (2019). <https://arxiv.org/abs/1806.07366>
- [42] Finlay, C., Jacobsen, J.-H., Nurbekyan, L., Oberman, A.M.: How to train your neural ODE: the world of Jacobian and kinetic regularization (2020). <https://arxiv.org/abs/2002.02798>
- [43] Greydanus, S., Dzamba, M., Yosinski, J.: Hamiltonian Neural Networks (2019). <https://arxiv.org/abs/1906.01563>
- [44] Cranmer, M., Greydanus, S., Hoyer, S., Battaglia, P., Spergel, D., Ho, S.: Lagrangian Neural Networks (2020). <https://arxiv.org/abs/2003.04630>
- [45] Lutter, M., Ritter, C., Peters, J.: Deep Lagrangian Networks: Using Physics as Model Prior for Deep Learning (2019). <https://arxiv.org/abs/1907.04490>
- [46] Kumar, R., Bhattacharyya, S.N.: One-sided finite-difference approximations suitable for use with richardson extrapolation. *J. Comput. Phys.* **219**, 13–20 (2006)
- [47] Tancik, M., Srinivasan, P.P., Mildenhall, B., Fridovich-Keil, S., Raghavan, N., Singhal, U., Ramamoorthi, R., Barron, J.T., Ng, R.: Fourier Features Let Networks Learn High Frequency Functions in Low Dimensional Domains (2020). <https://arxiv.org/abs/2006.10739>
- [48] Lienen, M., Lüdke, D., Hansen-Palmus, J., Günemann, S.: From Zero to Turbulence: Generative Modeling for 3D Flow Simulation (2024). <https://arxiv.org/abs/2306.01776>
- [49] Takamoto, M., Praditia, T., Leiteritz, R., MacKinlay, D., Alesiani, F., Pflüger, D., Niepert, M.: PDEBENCH: An Extensive Benchmark for Scientific Machine Learning (2024). <https://arxiv.org/abs/>

2210.07182

- [50] Ohana, R., McCabe, M., Meyer, L., Morel, R., Agocs, F.J., Beneitez, M., Berger, M., Burkhart, B., Dalziel, S.B., Fielding, D.B., Fortunato, D., Goldberg, J.A., Hirashima, K., Jiang, Y.-F., Kerswell, R.R., Maddu, S., Miller, J., Mukhopadhyay, P., Nixon, S.S., Shen, J., Watteaux, R., Blancard, B.R.-S., Rozet, F., Parker, L.H., Cranmer, M., Ho, S.: The Well: a Large-Scale Collection of Diverse Physics Simulations for Machine Learning (2024). <https://arxiv.org/abs/2412.00568>

- [51] Oommen, V., Bora, A., Zhang, Z., Karniadakis, G.E.: Integrating Neural Operators with Diffusion Models Improves Spectral Representation in Turbulence Modeling (2024). <https://arxiv.org/abs/2409.08477>

- [52] Li, H., Xu, Z., Taylor, G., Studer, C., Goldstein, T.: Visualizing the Loss Landscape of Neural Nets (2018). <https://arxiv.org/abs/1712.09913>